Available online at www.sciencedirect.com
ScienceDirect
Mendeleev Commun., 2024, **34**, 828–830

Mendeleev Communications

Synthesis, structure and properties of spin-labeled photosensitive chromone derivative

Kirill V. Agliulin,[a,b] Andrey V. Stepanov,[a] Vladimir N. Yarovenko,[a] Mikhail M. Krayushkin,*[a] Evgeny V. Tretyakov,[a] Darina I. Nasyrova,[a] Valentina V. Ilyushenkova,[a] Anton O. Ayt[b] and Tatyana M. Valova[b]

[a] *N. D. Zelinsky Institute of Organic Chemistry, Russian Academy of Sciences, 119991 Moscow, Russian Federation. E-mail: orgchem@mail.ru*
[b] *National Research Center 'Kurchatov Institute', 119421 Moscow, Russian Federation*

DOI: 10.1016/j.mencom.2024.10.019

A new hybrid chromone derivative bearing α-bromofuryl, *p*-(iminomethyl)benzoyl and 2,2,6,6-tetramethylpiperidin-1-oxyl moieties was synthesized by the azomethine reaction involving 4-amino-TEMPO. The benzoyl moiety in this paramagnetic molecule is almost perpendicular to the chromone plane. Having been exposed to UV light, this paramagnet undergoes a transformation accompanied by appearance of intense absorption and luminescence bands with maxima at 420 and 500 nm, respectively, *i.e.*, the presence of paramagnetic moiety does not interfere with generation of fluorescence.

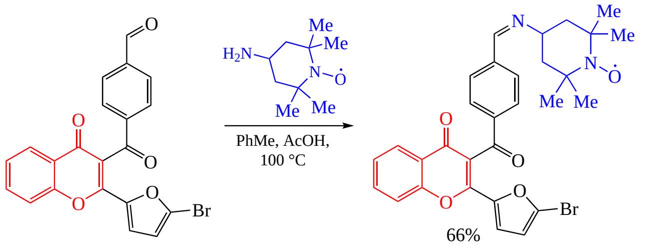

Keywords: stable radicals, nitroxides, chromones, photorearrangements, luminescence.

Chromones are widespread in nature and show a broad range of biological activity; their synthetic derivatives serve as active ingredients in numerous pharmaceuticals.[1–3] They are photoactive and readily participate in both reversible and irreversible photoinduced reactions. Previously, using numerous examples we studied UV light-induced photocyclizations of 3-acyl-2-furyl- or 3-acyl-2-thienylchromones **I** to derivatives **II** (Scheme 1).[4–6] The most interesting result is that the parent compounds **I** exhibit no fluorescence whereas the photoisomerization products, in contrast, fluoresce with relatively high quantum yields. Efficient photoconversion of **I** to give luminescent products **II** makes them applicable for advanced high-density data recording technologies. For example, prototypes of optical disks for single and high-density data storage with the possibility of multiple reading (WORM) based on substituted 3-acyl-2-hetarylchromones **I** were developed at the Zelinsky Institute of Organic Chemistry of RAS and the Photochemistry Center of RAS.[7]

An important feature of 3-acyl-2-hetarylchromones **I** that determines the possibility of their efficient operation in optical storage devices is the fluorescence quantum yield of photoisomerization products. These compounds have a closed electron shell; this means that the theoretical upper limit of internal quantum efficiency for them is only 25% because of the non-radiative energy loss of triplet excitons.[8] One way for crucial increase in the quantum yield is to introduce a paramagnetic group into the fluorophore molecule, because in this case luminescent emission would be caused by transitions from the doublet excited state to the doublet ground state, *i.e.*, by spin-allowed transitions. Following this strategy, we developed highly efficient organic luminescent materials that demonstrated quantum yields of up to 99% and, in addition, possessed high photostability due to the inversion of the singly occupied and highest occupied molecular orbitals.[9–12] Meanwhile, some publications noted that the presence of nitroxide radicals in nitroxide fluorescent systems can suppress fluorescence.[13] The idea and specific nature of our research is to design spin-labeled 3-acyl-2-hetarylchromones **I** that would be converted, upon photoisomerization, to annulated chromenones **II** with efficient (nearly 100%) luminescence in the visible region. It is evident that to reach this goal, it is necessary to obtain a broad range of chromones carrying various paramagnetic substituents and then to elucidate the structure–property relationships. This paper, describing the synthesis, properties, and photochemical behavior of the first hybrid spin-labeled chromone, serves as the starting point.

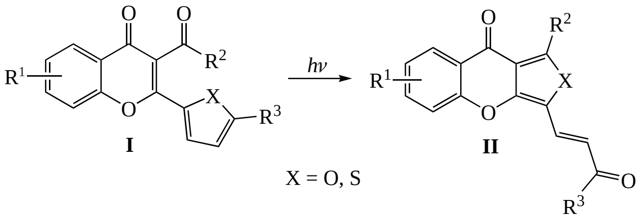

Scheme 1

The synthetic sequence is outlined in Scheme 2. The treatment of *o*-hydroxyacetophenone **1** with 4-(1,3-dioxolan-2-yl)benzoyl chloride **2** gave initially the intermediate *O*-acylation product whose rearrangement led to diketone **3**. Its further condensation with bromofurfural **4** afforded compound **5** (existing in solutions as a mixture of acyclic and cyclic forms **5a** and **5b**). This mixture was oxidized with selenium dioxide in dioxane at 65 °C to give chromone **6** with acetal protecting group untouched. When the oxidation of compounds **5a**,**b** was carried out at elevated

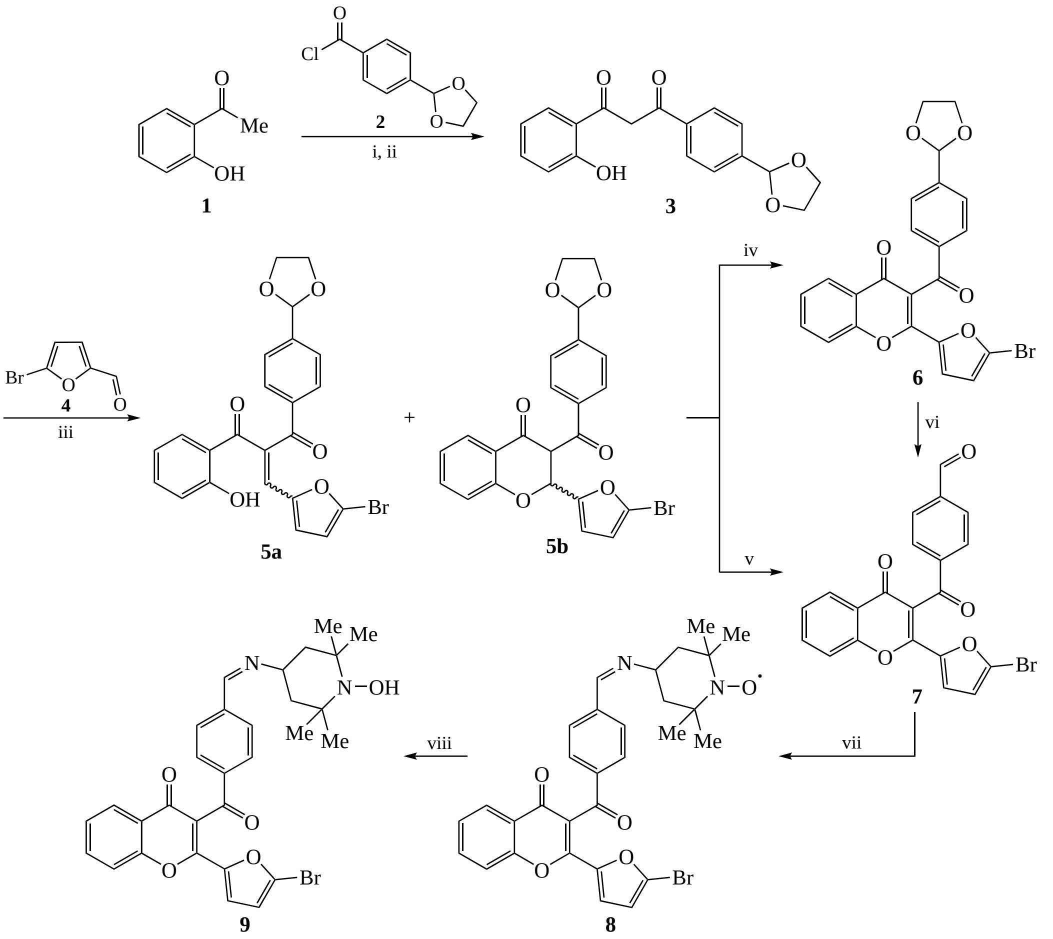

Scheme 2 *Reagents and conditions*: i, Py; ii, KOH, Py; iii, piperidine, EtOH; iv, SeO_2, 65 °C, dioxane, 12 h; v, SeO_2, dioxane, reflux, 24 h; vi, PTSA, acetone, 12 h; vii, 4-amino-TEMPO, PhMe, AcOH, 100 °C, 4 h; viii, $PhNHNH_2$, $CHCl_3$.

temperature (100 °C) for 24 h, the reaction ended in the formation of 4-[2-(5-bromofuran-2-yl)-4-oxo-4*H*-chromene-3-carbonyl]-benzaldehyde **7**, *i.e*., both the oxidation and the removal of the acetal protecting group took place. At the last stage, the heating of aldehyde **7** with 4-amino-TEMPO in toluene in the presence of a catalytic amount of acetic acid delivered the target spin-labeled chromone **8**. The molecular and crystal structures of **8** were determined by X-ray diffraction analysis. The purity of the paramagnetic phase was confirmed by spectroscopic data as well as by the NMR spectrum of hydroxylamine **9**, resulting from reduction of **8** with phenylhydrazine.

According to X-ray diffraction data of **8**,† the C(26)–O(4) and C(18)–C(19) bond lengths are 1.233 and 1.358 Å, which is typical of chromones (Figure 1). The furan ring lies nearly in the plane of the chromone nucleus. Conversely, the benzoyl group is orthogonal to the plane of chromone, as indicated by the O(2)–C(17)–C(18)–C(19) torsion angle equal to 87.8°. The C(7)–N(2) imine moiety is in the plane of the aromatic ring. The nitroxide bond length is typical and amounts to 1.299 Å.[14]

The electronic absorption spectrum of chromone **7** exhibits bands with maxima at 262 and 315 nm, but no absorption in the visible region is present. UV irradiation of chromone **7** induces its transformation to products resulting in an absorption band in the visible region with a maximum at 425 nm (the structure of photorearrangement products will be the subject of a separate publication) and an intense luminescence band with a maximum at 490 nm (Figure 2).

Paramagnetic chromone derivative **8** is also converted under UV irradiation, as indicated by the appearance of an intense

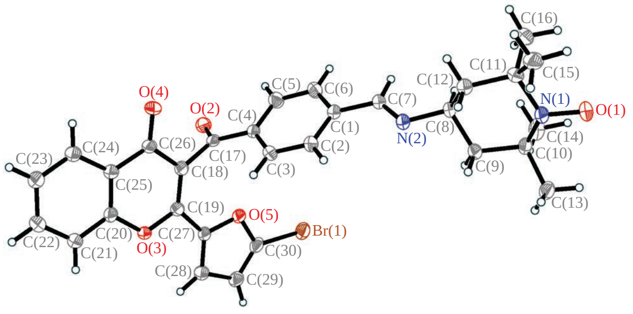

Figure 1 Molecular structure of spin-labeled chromone **8**.

---

† *Crystal data for* **8**. $C_{30}H_{28}BrN_2O_5$ (M = 576.45), orthorhombic, space group *Pbca*, at 100.00(10) K, a = 10.12010(10), b = 20.61980(10) and c = 25.3495(2) Å, Z = 8, d_{calc} = 1.448 mg m^{-3}, V = 5289.79(7) Å^3, μ(MoKα) = 2.477 mm^{-1}, F(000) = 2376. A total of 58954 reflections were collected (5737 independent reflections, R_{int} = 0.0489), GOOF 1.137, final R indices [$I > 2\sigma(I)$]: R_1 = 0.0708 and wR_2 = 0.1858, R indices (all data): R_1 = 0.0718 and wR_2 = 0.1868. Crystallographic data were collected on a Rigaku Synergy S diffractometer equipped with a HyPix6000HE area-detector (kappa geometry, shutterless ω-scan technique), using λ(CuKα) = 1.54184 Å. The intensity data were integrated and corrected for absorption and decay by the CrysAlisPro program.[15] The structure was solved by direct methods using SHELXT[16] and refined on F^2 using SHELXL-2018[17] in the OLEX2 program.[18] All non-hydrogen atoms were refined with individual anisotropic displacement parameters. All hydrogen atoms were placed in ideal calculated positions and refined as riding atoms with relative isotropic displacement parameters. A rotating group model was applied for methyl groups.

CCDC 2353872 contains the supplementary crystallographic data for this paper. These data can be obtained free of charge from The Cambridge Crystallographic Data Centre *via* https://www.ccdc.cam.ac.uk.

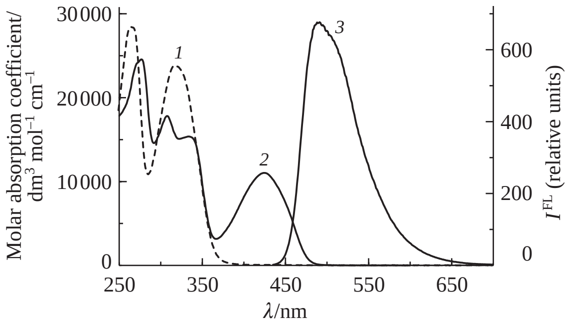

Figure 2 Absorption (*1*, *2*) and luminescence (*3*) spectra of compound **7** in acetonitrile before (*1*) and after (*2*, *3*) UV irradiation through a UFS-1 filter for 1.5 min; the luminescence spectrum was recorded upon excitation at 425 nm.

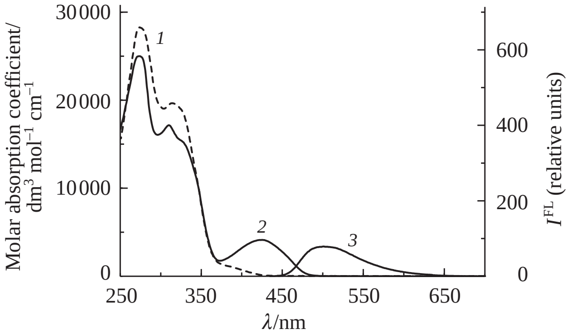

Figure 3 Absorption (*1*, *2*) and luminescence (*3*) spectra of compound **8** in acetonitrile before (*1*) and after (*2*, *3*) UV irradiation through a UFS-5 filter for 5 min; the luminescence spectrum was recorded upon excitation at 425 nm.

visible absorption band with a maximum at 420 nm and a luminescence band with a maximum at 500 nm (Figure 3). Attention is attracted by the fact that the presence of radical leads to a decrease in the luminescence intensity by almost an order of magnitude (but not to disappearance) and to a 10 nm red shift in comparison with chromone **7**.

In conclusion, we performed the first synthesis of a spin-labeled photosensitive chromone derivative, 2-(5-bromo-2-furyl)-3-(4-{(*E*)-[(1-oxyl-2,2,6,6-tetramethylpiperidin-4-yl)-imino]methyl}benzoyl)-4*H*-chromen-4-one. The molecular and crystal structures of this paramagnetic compound were determined by X-ray diffraction analysis. It was shown that the paramagnetic chromone derivative, like the diamagnetic precursor, is transformed upon UV irradiation, giving rise to an intense absorption band and luminescence band in the visible region. The formation of luminescent products upon isomerization of non-luminescent spin-labeled structures is a unique phenomenon that requires a separate study of structure–property relationships for this type of molecules.

Crystal structure determination was performed in the Department of Structural Studies of Zelinsky Institute of Organic Chemistry, Moscow.

Online Supplementary Materials

Supplementary data associated with this article can be found in the online version at doi: 10.1016/j.mencom.2024.10.019.

References

1 N.-ul-A. Mohsin, M. Irfan, S. ul Hassan and U. Saleem, *Pharm. Chem. J.*, 2020, **54**, 241; https://doi.org/10.1007/s11094-020-02187-x.

2 Z. S. Senobari, M. M. Hosseini, M. B. Teimouri, A. H. Rezayan, S. Samarghandian and A. Hekmat, *BMC Res. Notes*, 2023, **16**, 224; https://doi.org/10.1186/s13104-023-06508-7.

3 P. Kavitha and K. L. Reddy, *Arab. J. Chem.*, 2016, **9**, 640; http://dx.doi.org/10.1016/j.arabjc.2013.06.018.

4 V. A. Barachevsky, O. I. Kobeleva, A. O. Ayt, A. M. Gorelik, T. M. Valova, M. M. Krayushkin, V. N. Yarovenko, K. S. Levchenko, V. V. Kiyko and G. T. Vasilyuk, *Opt. Mater.*, 2013, **35**, 1805; http://doi.org/10.1016/j.optmat.2013.03.005.

5 O. I. Kobeleva, T. M. Valova, V. A. Barachevsky, I. S. Semenova, K. S. Levchenko, V. N. Yarovenko and M. M. Krayushkin, *Opt. Spectrosc.*, 2013, **114**, 401; https://doi.org/10.1134/S0030400X13020112.

6 Yu. Martynov, V. A. Barachevsky, A. O. Ayt, O. I. Kobeleva, T. M. Valova, K. S. Levchenko, V. N. Yarovenko and M. M. Krayushkin, *Opt. Mater.*, 2014, **37**, 488; http://doi.org/10.1016/j.optmat.2014.07.011.

7 V. Barachevsky, M. Krayushkin and V. Kiyko, in *Photon-Working Switches*, eds. Y. Yokoyama and K. Nakatani, Springer Japan KK, 2017, ch. 9, pp. 181–208; https://doi.org/10.1007/978-4-431-56544-4_9.

8 Y. Cao, I. D. Parker, G. Yu, C. Zhang and A. J. Heeger, *Nature*, 1999, **397**, 414; https://doi.org/10.1038/17087.

9 X. Ai, E. W. Evans, S. Dong, A. J. Gillett, H. Guo, Y. Chen, T. J. H. Hele, R. H. Friend and F. Li, *Nature*, 2018, **563**, 536; https://doi.org/10.1038/s41586-018-0695-9.

10 A. Abdurahman, T. J. H. Hele, Q. Gu, J. Zhang, Q. Peng, M. Zhang, R. H. Friend, F. Li and E. W. Evans, *Nat. Mater.*, 2020, **19**, 1224; https://doi.org/10.1038/s41563-020-0705-9.

11 Z. X. Chen, Y. Li and F. Huang, *Chem.*, 2021, **7**, 288; https://doi.org/10.1016/j.chempr.2020.09.024.

12 E. V. Tretyakov, in *Organic Radicals*, eds. C. Wang, A. Labidi and E. Lichtfouse, Elsevier, 2024, ch. 5, pp. 61–181; https://doi.org/10.1016/B978-0-443-13346-6.00005-1.

13 J. P. Blinco, K. E. Fairfull-Smith, B. J. Morrow and S. E. Bottle, *Aust. J. Chem.*, 2011, **64**, 373; https://doi.org/10.1071/CH10442.

14 E. V. Tretyakov and V. I. Ovcharenko, *Russ. Chem. Rev.*, 2009, **78**, 971; https://doi.org/10.1070/RC2009v078n11ABEH004093.

15 *CrysAlisPro, Version 1.171.41*, Rigaku Oxford Diffraction, 2021.

16 G. M. Sheldrick, *Acta Crystallogr.*, 2015, **A71**, 3; http://doi.org/10.1107/S2053273314026370.

17 G. M. Sheldrick, *Acta Crystallogr.*, 2015, **C71**, 3; http://doi.org/10.1107/S2053229614024218.

18 O. V. Dolomanov, L. J. Bourhis, R. J. Gildea, J. A. K. Howard and H. Puschmann, *J. Appl. Crystallogr.*, 2009, **42**, 229; http://doi.org/10.1107/S0021889808042726.

Received: 28th May 2024; Com. 24/7508